

UPGRADED BEAM PROFILE MONITORING USING CHROMOX AND FIBER OPTIC IMAGING FOR HIGH-RADIATION ENVIRONMENTS

A. Gottstein*, S. Braccini, L. Eggimann, E. Kasanda, I. Mateu
AEC, LHEP, University of Bern, Bern, Switzerland

Abstract

We present an upgraded beam monitoring system designed for use in high-radiation environments where conventional imaging solutions rapidly degrade. In the presented device, the radiation-sensitive P47 phosphor screen of the previous system is replaced with a radiation-hard Chromox ceramic scintillator, and the CMOS camera is relocated outside the irradiation zone by transmitting the optical signal through a 20-meter radiation-tolerant fiber optic bundle. To enhance operational flexibility, a pneumatic actuator enables remote insertion and retraction of the scintillating screen into the beam path. The radiation hardness of the Chromox ceramic and the fiber bundle was evaluated, and the optical system's resolution and fidelity were characterized. The new setup demonstrated stable imaging performance under irradiation, solving the frequent maintenance issues of the previous system. These improvements offer a robust and low-maintenance solution for beam profile monitoring in high-radiation accelerator environments.

INTRODUCTION

At the Bern Medical Cyclotron (BMC) laboratory, an 18 MeV proton beam is available for both routine radioisotope production and multidisciplinary research through a dedicated Beam Transfer Line (BTL) [1]. To support these activities, our group has developed a series of devices for beam diagnostics, such as the now commercialised UniBEAM detector [2], and, in collaboration with TRIUMF, an array of scintillators for non-destructive beam monitoring through the detection of secondary radiation surrounding the beamline [3]. More recently, the two-dimensional beam profiler π^2 [4] was implemented as a standard diagnostic tool, providing reliable information on beam profiles and intensities with minimal perturbation of the beam.

A new upgraded system has been realised, aimed at extending the operational range of the π^2 detector and improving its robustness under demanding irradiation conditions. We present the design and performance of the upgraded device, with a focus on the characterization of the response of its components under high proton fluxes and its long-term stability. The results confirm the suitability of this instrument for routine use in radioisotope production research and in dedicated irradiation studies, while also highlighting its potential for broader applications in beam diagnostics.

* alexander.gottstein@unibe.ch

THE π^2 UPGRADE

The first iteration of the π^2 beam monitoring device [4] proved effective for beam imaging but presented several limitations for routine operation. The P47 scintillator layer lacked mechanical stability, showing adhesion issues and progressive degradation over time. In addition, the camera positioned close to the scintillating screen suffered radiation damage from secondary radiation, leading to frequent replacements due to the accumulation of dead pixels.

To overcome these drawbacks, an upgraded design was developed (see Fig. 1). The P47 layer was replaced by a 500 μm -thick Chromox ceramic (Al_2O_3 doped with chromium oxide, manufactured by Advatech), offering superior mechanical robustness and long-term stability under irradiation. To mitigate camera damage, the readout was relocated outside the irradiation zone by coupling the scintillator to a 20 m ESKA™ FF-VK80 optical fiber bundle, which guides the image to a radiation-protected area.

Since the Chromox ceramic and its aluminium holder fully stop the 18 MeV proton beam, a pneumatic actuator was integrated to enable remote insertion and retraction of the scintillator, making the system a destructive monitor. Dedicated lens systems are employed to focus the scintillation image onto the fiber input and to project the fiber output onto a commercial CMOS camera (CS165CU1/M Zelux®).

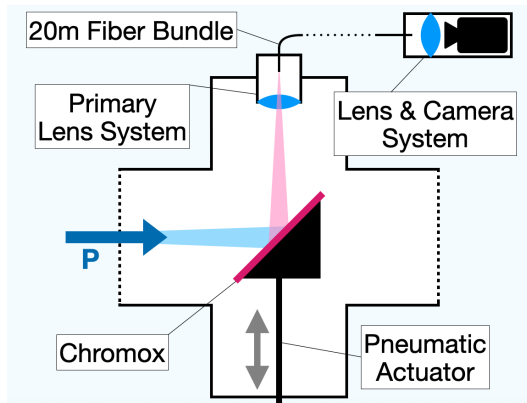


Figure 1: Schematic of the upgraded π^2 beam monitoring device. The Chromox scintillator is mounted on a pneumatic actuator and read out via a primary lens system, a 20 m optical fiber bundle, and a remote lens-camera system.

Prior to installation on the beam line, the device was assembled and tested in the laboratory using an LCD screen placed at the position of the Chromox scintillator. This procedure enabled a precise calibration of the optical system, which requires a geometric correction due to the inclination

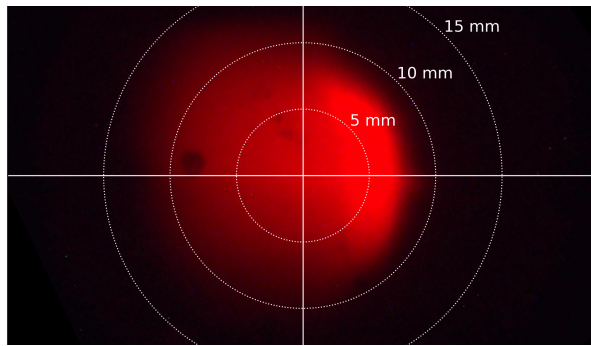


Figure 2: A proton beam interacts with the Chromox during the focusing process. After a geometric correction of the recorded image, the proton beam's position, size, and profile can be extracted from the image delivered by the upgraded π^2 . The dark spots originate from stains on the fiber's tip.

of the scintillator plane with respect to the fiber bundle. By recording a reference grid displayed on the LCD screen, the transformation matrix for the perspective correction was determined. This calibration allows the extraction of the beam position, size, and profile from the scintillation image of the Chromox. An example of a corrected image of a semi-focused proton beam, recorded with the upgraded π^2 setup, is shown in Fig. 2.

COMPONENT TESTS

To ensure the long-term reliability of the upgraded device, dedicated tests were carried out on its key components. In particular, the radiation hardness of the Chromox scintillator and the optical fiber bundle was investigated under high proton fluences. For the Chromox screen, the test conditions directly reproduce the operational environment, since the ceramic is exposed to the full proton beam during measurements. The fiber bundle, on the other hand, is expected to receive only secondary radiation (mainly neutrons and gamma rays) in routine operation. Nevertheless, a direct proton irradiation test was performed to assess its robustness to large accumulated doses of radiation.

Chromox Radiation Hardness

The radiation hardness of Chromox was evaluated by monitoring its scintillation light output under irradiation with an 18 MeV proton beam. The initially flat beam was collimated to a circular spot of 4 mm diameter before being extracted into air and directed onto the Chromox sample. The beam intensity was measured upstream with a secondary electron monitor (SEM), while a movable Faraday cup (FC) located between the SEM and the extraction window provided an absolute reference measurement when inserted.

The light emission from the Chromox was detected with a *Thorlabs PDA36A-EC Si Amplified Detector*, positioned at a 45° angle relative to the ceramic surface, as shown in Fig. 3. The diode signal was normalized to the SEM reading and is shown as a function of the integrated proton flux in Fig. 4.

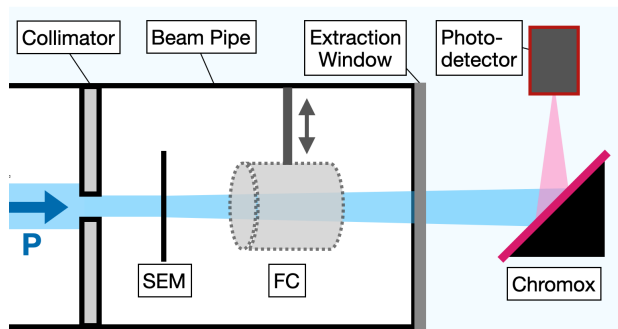


Figure 3: Experimental setup for the Chromox radiation hardness test. The proton beam is collimated and monitored with a SEM and a movable Faraday Cup (FC) before extraction into air. The light emitted by the Chromox scintillator is detected by a photodiode.

The measurement campaign was conducted in two sessions on separate days. To mitigate potential beam drifts during long-term irradiation at the BTL, the linearity of the SEM with respect to both the FC and the diode detector was verified before and after each session. The diode current was then normalized to the drift-corrected SEM signal, ensuring proportionality to the extracted beam current interacting with the Chromox. The resulting data were scaled to the maximum recorded value for presentation. From the SEM-FC calibration, the integrated proton flux was derived and used as the x-axis in Fig. 4.

During the first irradiation session, the signal exhibited fluctuations of up to $\pm 1\%$, primarily caused by unstable beam conditions that required frequent re-centering and flattening of the proton beam using the BTL steering and quadrupole magnets. Adjustments to the beam steering and focusing led to small displacements of the beam spot on the Chromox, which in turn influenced the detected light output but were not reflected in the SEM measurement. In the second session, the beam required less frequent steering interventions; however, long-term drifts most likely introduced similar effects, albeit at a reduced level.

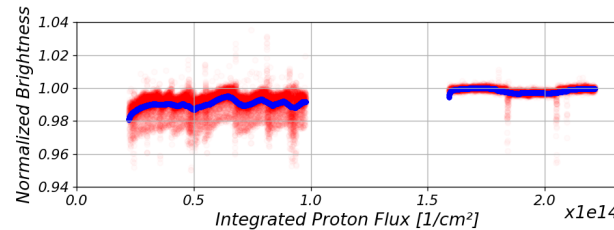


Figure 4: Normalized light output of the Chromox scintillator as a function of the integrated proton flux. Red points represent individual measurements, while the blue curve shows a 5-minute moving average.

Fiber Bundle Radiation Hardness

The fiber bundle transmits the image from the Chromox scintillator to the CMOS camera. Since parts of the bundle

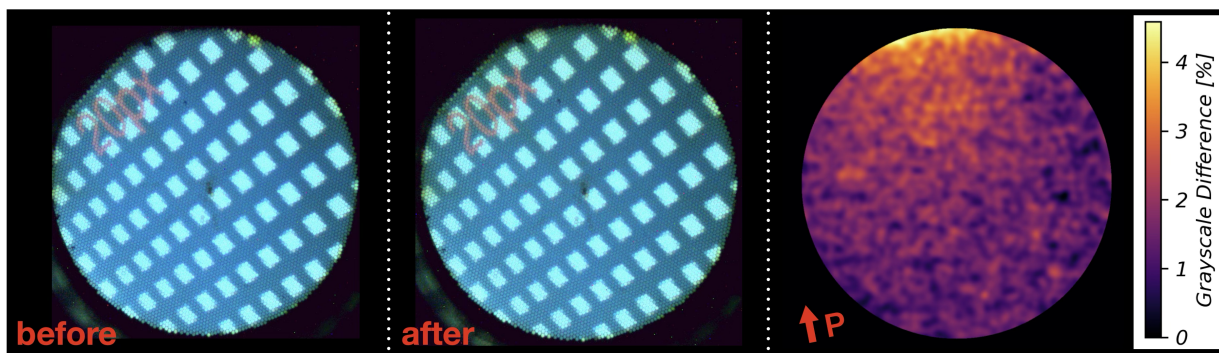


Figure 5: Test grid on the LCD screen recorded by the CMOS camera before (left) and after (middle) the fiber bundle irradiation. On the right the induced relative grayscale difference is shown. The red arrow shows the proton beam direction.

are located in radiation-rich regions, they may be subject to damage from secondary particles such as neutrons and gamma rays. In this work, we tested the fiber bundle's performance while directly exposing a 4 cm part of it to 14.3 MeV protons. For this test, a mock set-up has been installed away from the beam, where instead of the Chromox screen a small LCD screen was employed. During the irradiation, a series of test images depicting different black and white grids was monitored. Due to the 2 mm diameter of the beam and the relatively low energy of the proton beam, the dose distribution within the fiber bundle was not uniform. Using a TOPAS simulation, the dose distribution within the fiber bundle can be reconstructed, indicating that the entrance area from where the beam penetrates the fiber was exposed to around 43 kGy, whereas the exit area, due to Bragg peak effects, was exposed to around 216 kGy.

The nonuniformity of the dose distribution is also visible in Fig. 5, where the relative grayscale value difference of the before and after irradiation test picture is plotted. The area that underwent the strongest change shows a 4.5 % change of the relative grayscale. It is where the Bragg peak of the 14.3 MeV protons is located.

DISCUSSION AND OUTLOOK

The radiation hardness tests carried out on the key components of the upgraded π^2 device yielded promising results. The Chromox scintillator showed no measurable degradation of its light output up to an accumulated fluence of approximately 2.2×10^{14} protons/cm², corresponding to about one year of typical operation at the BMC.

The optical fiber bundle exhibited a slight reduction in transmission after exposure to a proton dose of approximately 216 kGy. This level is expected to be well above the annual dose from secondary radiation (neutrons and gamma rays) under standard operating conditions. However, since no detailed model of the secondary radiation distribution along the beam line is currently available, further studies are required to quantify the fiber's long-term performance under realistic conditions. In particular, dedicated irradiations with neutrons and gamma rays would provide valuable input for estimating the operational lifetime of the fiber bundle.

A more detailed characterization of the Chromox ceramic is also foreseen. Future studies should include investigations

of spatial uniformity and response linearity, with the goal of enabling fully quantitative measurements of the beam profile and intensity after a calibration. These efforts will further consolidate the upgraded π^2 as a robust and versatile diagnostic tool for research at the BMC and for broader applications in accelerator beam instrumentation.

CONCLUSION

The upgraded π^2 detector has demonstrated reliable performance and shows strong potential for routine use in the research activities carried out at the Bern Medical Cyclotron. A key improvement over the previous design is the relocation of all radiation-sensitive components outside the irradiation zone, achieved through the use of an optical fiber bundle for image transmission. This ensures long-term stability and allows the device to remain permanently installed on the beam line. When not in use, the Chromox scintillator can be retracted from the beam path by means of the pneumatic actuator, enabling flexible operation without interfering with other experiments.

ACKNOWLEDGEMENTS

We are grateful for the contributions of the LHEP engineering and technical staff (Silas Bosco, Finn Tschan, and Efraim Elsholtz in particular for this work). This research was partially funded by the Swiss National Science Foundation (SNSF). Grants: IZURZ2_224901 and CRSIIS_180352.

REFERENCES

- [1] S. Braccini, "The new Bern PET cyclotron, its research beam line, and the development of an innovative beam monitor detector", *AIP Conf. Proc.*, vol. 1525, no. 1, pp. 144–150, Apr. 2013, doi:[10.1063/1.4802308](https://doi.org/10.1063/1.4802308)
- [2] M. Auger *et al.*, "Accelerator and detector physics at the Bern medical cyclotron and its beam transport line", *Nukleonika*, vol. 61, no. 1, pp. 11–14, Mar. 2016, doi:[10.1515/nuka-2016-0009](https://doi.org/10.1515/nuka-2016-0009)
- [3] S. Usherovich *et al.*, "A novel fiber-optic beam monitor", *J. Phys.: Conf. Ser.*, vol. 2687, no. 7, p. 072003, Jan. 2024, doi:[10.1088/1742-6596/2687/7/072003](https://doi.org/10.1088/1742-6596/2687/7/072003)
- [4] S. Braccini *et al.*, "A Two-Dimensional Non-Destructive Beam Monitoring Detector for Ion Beams", *Appl. Sci.*, vol. 13, no. 6, p. 3657, Mar. 2023, doi:[10.3390/app13063657](https://doi.org/10.3390/app13063657)